Hindawi
Advances in Meteorology
Volume 2017, Article ID 8971236, 11 pages
https://doi.org/10.1155/2017/8971236

Research Article

A Study on Parameterization of the Beijing Winter Heavy Haze Events Associated with Height of Pollution Mixing Layer

Tao Niu, Jizhi Wang, Yuanqin Yang, Yaqiang Wang, and Cheng Chen

Atmospheric Composition Observing & Service Center, Chinese Academy of Meteorological Sciences, Beijing 100081, China

Correspondence should be addressed to Jizhi Wang; jzwang@cma.gov.cn

Received 14 August 2017; Accepted 23 November 2017; Published 19 December 2017

Academic Editor: Jiyi Lee

North China Plain, Beijing, Tianjin, and Hebei province are the major areas facing the decreasing air quality and frequent pollution events in the recent years. Identifying the effect of meteorological conditions on changes in aerosol concentration and the mechanism for forming such heavy pollution in North China Plain has become the focus of scientific research. The influence of atmospheric boundary layer characteristics on air quality has become the focus of attention and research. However, the boundary layer describes that the influences of air pollution have sometimes been duplicated and confused with each other in some of the studies. It is necessary to pay attention to some extent, raising awareness of related pollution mixing layer. The conclusions of the study include the following: (1) The lowered height of pollution mixing layer (H_PML) was favorable for the increase of the $PM_{2.5}$ density. The lowered height of pollution mixing layer had significant impacts on formation of severe haze. (2) A statistical analysis of large-scale heavy pollution cases in eastern China shows that the H_PML parameters have significant contributions. (3) The feedback effect of the high value of the convection inhibition (CIN), which is unfavorable to vertical diffusion of pollution, causes further reduction of H_PML, resulting in cumulative pollution again.

1. Introduction

In December 2016, the North China region witnessed a historically rare pollution event, including the widespread hazy weather across the Yellow River and Huai River basins. Just in 24 hours from 18 to 19 December, the total area under influence of the severe haze was doubled, covering more than a million square kilometers, affecting 12 provinces or municipalities, that is, Jilin, Liaoning, Beijing, Tianjin, Hebei, Shandong, Henan, Shaanxi, Shanxi, Hubei, Anhui, and Jiangsu. Consequently, the red warning signal for heavy air pollution was launched in Beijing. December 2016 ranked top in terms of pollution severity for more than a decade, and the winter haze in North China once again became a focus of public opinion.

Under the global change, the air quality in the Earth's atmosphere tends to be gradually aggravated. The Beijing-Tianjin-Hebei area is the major region that has been frequently affected by air pollution in the recent years [1, 2]. Emissions and weather conditions are two important factors for air quality. Such questions as how to identify the impacts of weather conditions on local aerosol accumulation and density including impacts of small- and microscale processes are commonly of interest but it is difficult to give a precise answer. Efforts have been made to select some meteorological elements from the common weather parameters to analyze their contributions to possible changes in air quality, and their contributions sometimes are mutually offset and even contradictory [3, 4] due to complexity of mechanisms. However, the objective and quantitative assessments on the impacts of changing weather conditions upon aggravation and mitigation of atmospheric aerosol pollution have become a focus of attention in research.

Progress has already been made in studies on numerical air quality modeling [5, 6]. The difficulty encountered in studies and predictions of chemistry models is that the worldwide emission inventories are not available in a timely manner, usually lagging far behind demand for predictions, hence restricting further improvements of operational predictability in this direction. The studies on identification of density variations of atmospheric particles including $PM_{2.5}$ and their impacts show that the hygrometric characteristics

Table 1: List of studying on the relationship between air pollution and boundary layer in recent years.

Abbreviation	Meaning of abbreviations	References
PBL	Planetary boundary layer	Hu et al. [9]; Wang et al. [14]; Zhang et al. [15]
ABL	Atmospheric boundary layer	Ao et al. [4]
SL	Superadiabatic layer	Haugen et al. [16]
ML	Mixed layer	Wallace and Hobbs [17]
CIL	Capping inversion layer	Wallace and Hobbs [17]; Ao et al. [4]
CBL	Convective boundary layer	Zhao [18]
RML	Residual mixed layer	Zhang et al. [19]; Ma et al. [20]

of different emission particles vary significantly under different atmospheric condensation conditions. The duration of maintaining a hygrometric process in adaptation to various atmospheric conditions also has significant impacts on particle density variations [7].

In his series of famous studies on parameterization, Kuo [8] first presented cloud physics, its microphysic processes, and large-scale observations in parameterization schemes, which have been widely used for numerical weather predictions since then. Research findings show that the parameterization allows "incomparably describable" atmospheric microphysics in "different magnitudes" to interact with large-scale processes and solving a bunch of relevant equations. Hu et al. present a comprehensive evaluation study to address the importance of PBL parameterization schemes in WRF-Chem predictions of particles with diameters less than 2.5 microns ($PM_{2.5}$) during February 2014 over the most polluted regions in China, where $PM_{2.5}$ concentrations higher than $500\,\mu g{\cdot}m^{-3}$ were observed [9]. In the recent years, encouraging results have been achieved on parameterization methodologies linking air quality and meteorological conditions. Some studies both at home and overseas [10–13] have presented a new advance in PLAM index methodology to characterize whether the aggravated meteorological conditions are favorable or not for aggravating local air pollution, hence providing an objective basis for identifying the correlation of meteorological conditions with aerosol density variations. This method has been widely recognized and used worldwide.

In this paper, our studies and analyses focus on characteristics of isentropic (iso-θe) processes based on PLAM index; the height of pollution mixing layer features and the vertical atmospheric structure are analyzed; the correlation of the PLAM sensitive parameter-condensation function (fc) with the height of pollution mixing layer is discussed; correlation and interactions of PLAM index with local aerosol density variations are both explored; and the mechanism for forming the heavy pollution or severe hazy weather event in December 2016 is also addressed.

2. Data and Methodology

2.1. Data. In this section, NCEP 2.5 × 2.5 reanalysis and automatic weather station (AWS) data, both conventional surface and upper air observations from the climate stations of the National Climate Center, are used for calculations to investigate any meaningful implication of PLAM index for aerosol pollution; the atmospheric vertical wind, temperature, and humidity fields in the process of the rarely heavy pollution in December 2016 are explored; the role of atmospheric environment to inhibit pollution dispersion is investigated; and the mechanism for forming heavy pollution in Beijing is also discussed.

2.2. Height of Pollution Mixing Layer. Hu et al. point out [9] that although the planetary boundary layer (PBL) parameterizations are critical to air quality modeling, but it is not well quantified that constraining the air quality simulations by PBL parameterization schemes under the heavy haze polluted boundary layer conditions. In recent years, many progresses of studies on the atmospheric boundary layer characteristics and their impact on the air pollution were made (see Table 1) [4, 9, 14–20]. However, the way with which boundary layer describes the influences of air pollution is easily duplicated and confused. For example, the planetary boundary layer (PBL) usually refers to the large-scale Ekman dynamic boundary layer [14–16]. So it is unreasonable to some extent, if the characteristic of the air pollution related to near-surface boundary layer is evaluated by using the concept of PBL.

For the heavy haze pollution measurement, one of selected functionalities of parameterization scheme is to judge whether an air mass over a specific locality satisfies the "static and stable" attribute or not.

It is known that θ_e is an important parameter that reflects such attribute of air masses (Yang et al., 1980) [21], and, with this attribute, the constant "homogeneity" of θ_e, that is, $d\theta_e/dt \approx 0$, can be used to express the basic physics for diagnosing meteorological conditions. The iso-θ_e process is also called an isentropic atmospheric process. According to the thermodynamic equation, such stable nature of large-scale circulation, the attribute with constant "homogeneity" of air masses, may be expressed as follows [13, 22]:

$$\begin{aligned} \mathrm{PLAM} &\propto \frac{d\theta_e}{dt} \propto \frac{\theta_e f_c}{C_p T}, \\ \theta_e &= \theta \exp\left[\left(\frac{L w_s}{C_p T}\right)\right], \\ \theta &= T\left[\left(\frac{1000}{P}\right)^{Rd/C_p}\right]. \end{aligned} \tag{1}$$

Expression (1) gives the basic equations to parameterize the "homogeneous" attribute (θ_e) of the air masses. T, θ_e, f_c, w_s, and C_p represent air temperature, equivalent wet potential temperature, condensation function, saturation mixing ratio, and specific heat at constant pressure, respectively. In expression (1) defining PLAM index, another important sensitive parameter is the condensation function f_c, which is the threshold for controlling growth of aerosol density. The reason for introducing this function is to judge whether the aerosol density "grows" or "dilutes," as f_c describes water vapor condensation, concentration of minute particles, and hygrometric process in the atmosphere. This paper gives an in-depth analysis of descriptive functionality of PLAM index, explores contributions of relevant PLAM sensitive parameters in the relatively "static and stable" isentropic processes, and investigates impacts of the height of pollution mixing layer and vertical atmospheric structure upon the local aerosol density variations.

In expression (1), according to the definition of the wet potential temperature θ_e, any layer in which the saturated mixing ratio is satisfied ($w = w_s$) can be considered as the saturated atmospheric stratification. As $R_d/C_p = 0.288$ in expression (1) is a constant value, in the isentropic (iso-θ_e) process, the air pressure is used to express the lifting condensation level (LCL), which provides favorable weather conditions to allow new aerosol particles to grow continuously in the hygrometric process of pollution emissions in combination with pollution mixing. Thus, when rain droplets have not yet reached the threshold of f_c, it is favorable for pollution mixing process to be sustained at this level, which is called the height of pollution mixing layer (H_PML). Using an iterative algorithm, H_PML can be derived in the following expression [23]:

$$\text{H\_PML} \approx 6.11 \times 10^2 \times \left(\frac{0.622 + 0.622\,(e_s/(p - e_s))}{0.622\,(e_s/(p - e_s))} \right). \quad (2)$$

Expression (2) presents the air pressure coordinates (P) as the height of pollution mixing layer.

2.3. Analysis on Atmospheric Thermodynamic Structure and Pollution Dispersion Inhibition. Studies show that when a "dirty" air parcel is warmer than its ambient air in the lower atmosphere, it will be lifted from its initial location or directly enter an ascending process of the wet adiabatic, and this "buoyancy" of the air parcel is contributed by the Convective Available Potential Energy (CAPE):

$$\text{CAPE} = R_d \int_{\text{EL}}^{\text{LFC}} \left(T_v' - T_v\right) d \ln p. \quad (3)$$

In expression (3), P is the air pressure, $T_v' - T_v$ gives the difference between the virtual temperature of the ascending parcel and virtual temperature of the environment. According to expression (3), CAPE can be calculated by integrating the "buoyancy" of the parcel from the level of free convection (LFC) to the equilibrium level (EL). On the temperature-entropy or T_LOGP chart, the total area covered by both atmospheric sounding curve of the environment (red solid line) and the ascending curve of adiabatic parcel of air pollutants (green line) indicates abundance or absence of the "instable energy" CAPE. When CAPE is negative, which is expressed in convective inhibition (CIN), both dispersion and ascending motion of pollutants will be inhibited. Some studies show that when the absolute CIN value is greater than 100 J·kg^{-1}, the dispersion will be inhibited substantially [17, 24].

2.4. Index Diagnosis of Pollution Transport at the Isentropic Surface. As it is known, both updraft and subsidence of dry or wet air are usually the most common and frequent air motions in the atmosphere. However, θ_e remains basically unchanged in either ascending or descending motion of air particles under a dry or wet condition [21]. In other words, the true trajectory of air particles can be obtained by analyzing and calculating airflows on the isentropic surface relative to their motions on the isentropic surface if the motion of an air parcel is observed from perspective of iso-θ_e. A relative airflow on the isentropic surface is expressed in the following equation [25–27]:

$$\vec{V} = \vec{V}_{\text{obs}} - \vec{V}_{\theta_e}, \quad (4)$$

where $\vec{V}_{\text{obs}}$ and $\vec{V}_{\theta_e}$ and are the observed wind vector and the movement vector of the isentropic surface (i.e., weather system), respectively. Usually, when rainfall and snowfall systems are discussed, some meaningful results can be achieved by analyzing air pressure (P), temperature (T), specific humidity (q), and relative airflow $\vec{V}$ on isentropic surface to track airflow trajectories on the iso-θ_e surface [27, 28]. Using expression (1), the weather elements P, T, and q are calculated to give the distribution of PLAM index and its variations on iso-θ_e surface are tracked to find out its transport trajectory. If the wind vector $\vec{V}$ of any arbitrary station around Beijing, which can be derived from expression (4), is projected onto the municipality as $\vec{V}'_{\to\text{BJ}}$, then the product of PLAM multiplied by $\vec{V}'_{\to\text{BJ}}$ on the isentropic surface can be used to express the pollution transport to Beijing from its surrounding areas [23]:

$$\text{PLAM}_{\to\text{BJ}} = \text{PLAM} \cdot \vec{V}'_{\to\text{BJ}}, \quad (5)$$

where a positive value of $\text{PLAM}_{\to\text{BJ}}$ represents the meteorological conditions that are favorable for pollution transport to Beijing from its surrounding areas, or vice versa, and the $\text{PLAM}_{\to\text{BJ}}$ value shows the intensity of the transport impact.

3. Findings and Discussions

3.1. Heavy Pollution Process in Beijing in the Period of 1–31 December 2016. Figure 1 presents the heights of pollution mixing layer which were calculated from expression (2) using day-by-day (hourly) $PM_{2.5}$ observations and synchronous

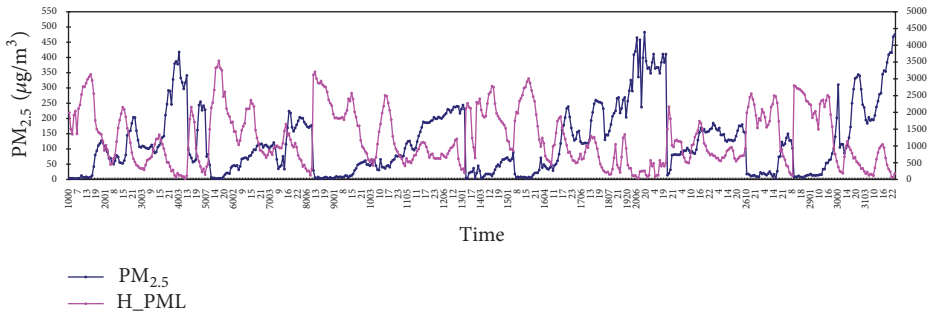

Figure 1: Hourly $PM_{2.5}$ observations and H_PML in Beijing in the period of 1–31 December (542 synchronous observations patterns).

data in Beijing in the period of 1–31 December 2016. Totally, there are 542 sets of synchronous observation layouts, as it is seen in Figure 1.

The $PM_{2.5}$ measurements and distribution of the heights of pollution mixing layer (H_PML) show that $PM_{2.5}$ and H_PML oscillate synchronously in the opposite phase. In whole December, there were 6 episodes in which significant $PM_{2.5}$ peaks were detected, occurring on 2~4, 7~8, 11~13, 16~21, 24~26, and 30~31 December, respectively. These high $PM_{2.5}$ values were 450, 250, 210, 500, 200, and 500 $\mu g/m^3$, respectively. Synchronously, 6 low H_PML values also appeared, and totally there were 6 fluctuations in the month, showing a 5-day oscillation cycle, a very interesting characteristic (Figure 1). The Explosive Growth Period of $PM_{2.5}$ concentration (EGP) seen in Figure 1 represents the episode of 16~21 December, in which the synchronous oscillation of $PM_{2.5}$ and H_PML in the opposite phase is the most typical.

3.2. Contribution of the Height of Pollution Mixing Layer. Figure 2 gives an analysis of day-by-day (hourly) $PM_{2.5}$ measurements relative to H_PML in the period of 1–31 December 2016. Figure 2 shows the following:

(1) In the frequent heavy pollution events that occurred in December 2016, H_PML was inversely correlated with $PM_{2.5}$ measurements. As stated in the above section, the episode of 16–21 December shown in the Explosive Growth Period of $PM_{2.5}$ concentration (EGP) in Figure 1 was most typical. At 08:00–14:00 on 15 December, H_PML reached its peak value, that is, 3000 m, but a low $PM_{2.5}$ value was measured in the same episode, which was less than 50. At 20:00 on 20 December, H_PML was less than 200 m, but $PM_{2.5}$ value peaked at 500 $\mu g/m^3$ (see Explosive Growth Period of $PM_{2.5}$ concentration (EGP) in Figure 1). Therefore, the height of pollution mixing layer has a universal impact on formation of severe haze.

(2) An inverse correlation exists between $PM_{2.5}$ and H_PML, and the confirmation coefficient of the negative correlation is $R^2 = 0.566$, with its significance level exceeding 0.001 (Figure 2). This shows that H_PML gives a good performance for diagnosing $PM_{2.5}$ density. The lower the H_PML is, the higher the accumulated $PM_{2.5}$ density will be.

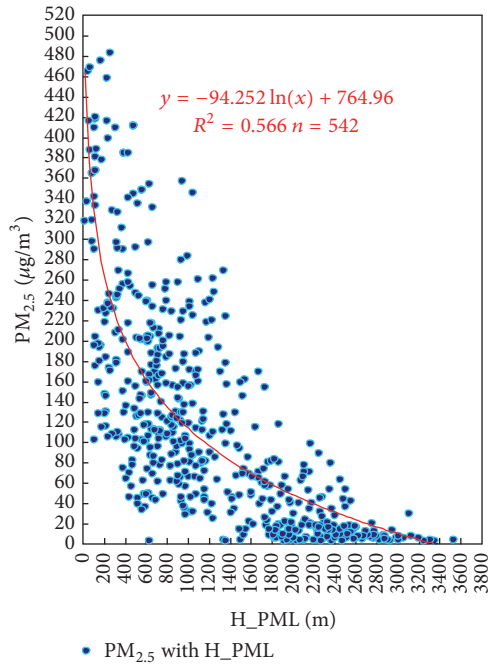

Figure 2: Analysis of hourly $PM_{2.5}$ measurements relative to H_PML in December 2016.

3.3. Contribution of Atmospheric Convective Inhibition to Heavy Pollution. As stated above, studies on vertical thermodynamic structure in the atmosphere show that CAPE is calculated by integrating the buoyancy of the air parcel from the level of free convection (LFC) to the equilibrium level (EL). When positive CAPE energy is obtained, convection develops and it is favorable for air pollution dispersion. On the contrary, when CAPE is negative, the convective dispersion of pollutants will be inhibited. The threshold values of convective dispersion or inhibition energies are given as follows [17]:

CAPE:

0000~1000 $J \cdot kg^{-1}$, lower bound of deep convection

1000~2500 $J \cdot kg^{-1}$, convection in medium intensity

2500~4000 $J \cdot kg^{-1}$, genesis of strong convection

≥4000 $J \cdot kg^{-1}$, genesis of extreme convection

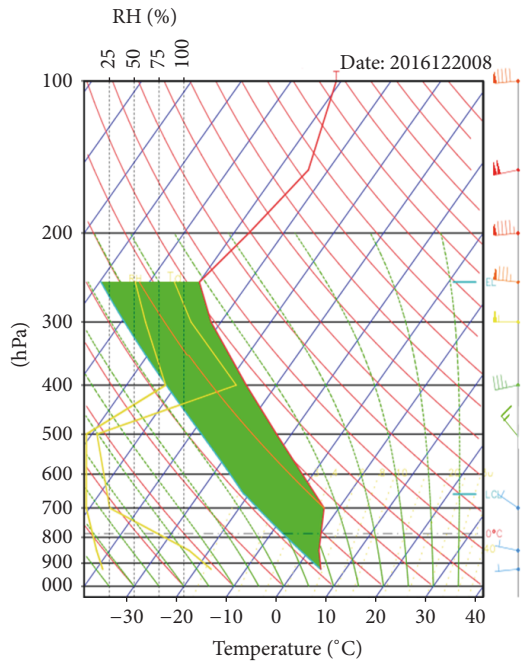

Figure 3: Vertical thermodynamic diagrams over Beijing on 20 December 2016.

The convective inhibition (CIN) refers to a negative CAPE value. If CIN is greater than 100 J·kg^{-1}, the aforementioned dispersion will be unlikely to occur without any external forcing.

Figure 3 presents vertical thermodynamic diagrams over Beijing at 08:00 on 20 December, which is prepared based on calculations according to expression (3), using air pressure (P), temperature (T), and dew point temperature (T_d) observations in Beijing.

At 08:00 on 20 December 2016, the air parcel LFC was displaced at 650 hPa; the mean temperature at this level was given in following formula: $T'_v - T_v = -6.66^\circ$C, which was derived from Figure 3. As it is revealed in this typical temperature-entropy diagram for 20 December 2016, just opposite to 16 December, the ascending curve T'_v along the iso-θ_e line was located on the left side of the stratification curve T_v but stayed away from the ambient sounding curve; the temperature of ascending air parcel T'_v was lower than its ambient temperature by 7°C ($T'_v - T_v = -6.66^\circ$C). According to expression (3), CAPE can be derived:

$$\begin{aligned} \text{CAPE} &= R_d \int_{\text{EL}}^{\text{LFC}} \left(T'_v - T_v\right) d \ln p \\ &= 287 \times -6.66 \times 2.72 = -5200 \text{ J·kg}^{-1}. \end{aligned} \tag{6}$$

As above calculation results show, at 08:00 on 16 December, CAPE value was −5200 J·kg^{-1}, whereas the inhibition energy (CIN) peaked at 5200 J·kg^{-1}, which was 50 times higher than the threshold and absolutely stable; the green zone in the thermodynamic diagram was expanding significantly. At this hour, $PM_{2.5}$ was soaring from 50 up to 500 μg/m^3 (see Explosive Growth Period of $PM_{2.5}$ concentration (EGP) in Figure 1), which was a 10-fold increase relative to the initial stage, and absolutely stable [17]. Obviously, CIN made a very significant contribution to the heavy pollution event in Beijing.

3.4. PLAM-Based Diagnosis on Meteorological Conditions for Pollution Transport to Beijing from Its Surrounding Areas. Figure 4(a) presents an analysis of the isentropic surface (θ_e = 280°k) for 08:00 on 20 December 2016 which was calculated using expressions (4) and (5), and it also shows the distribution of meteorological conditions for orienting pollution transport towards Beijing ($\text{PLAM}_{\rightarrow\text{BJ}}$) from its surrounding areas. It can be seen from Figure 4 that the Beijing-oriented (note: orientation target is changeable) red zones in the distribution chart indicate that the surrounding meteorological conditions are favorable for pollution transports in positive values towards Beijing. The blue zones show that the weather conditions are unfavorable for Beijing-oriented transports in negative values; in other words, the transports are not oriented to Beijing and even can be in an opposite direction.

Figures 4(b), 4(c), and 4(d) give the predicted $\text{PLAM}_{\rightarrow\text{BJ}}$ index distributions for 19 December 2016, which are calculated using expressions (4) and (5). The starting point of the forecast is: 08:00 on 19 December; the rolling forecast period is for 3 h (Figure 4(b)), 6 h (Figure 4(c)), and 12 h (Figure 4(d)), respectively. Comparing Figure 4(a) with Figure 4(b) and Figure 4(c) with Figure 4(d), we see the following:

(1) At 08:00 on 20 December 2016, the $\text{PLAM}_{\rightarrow\text{BJ}}$ index in Beijing area exceeded 300 (Figure 4(a)), which was consistent with the fact that $PM_{2.5}$ density reached 500 μg/m^3 in Beijing at this hour (also refer to Figure 1). It is shown that the meteorological conditions in Beijing fell into a worse category at this time, which were unfavorable for pollution dispersion in the lower atmosphere.

(2) As the 3 h prognosis chart (Figure 4(b)) shows, a small zone with high $\text{PLAM}_{\rightarrow\text{BJ}}$ index (greater than 100) is oriented to Beijing from the southern Hebei and western Shandong provinces.

(3) As it is indicated in the 6 h $\text{PLAM}_{\rightarrow\text{bj}}$ index prognosis chart (Figure 4(c)), the small high index value zone near southern Hebei extends in a south-north direction, and Beijing-oriented pollution transport is enhanced. The high index center has grown from 100 to more than 200. Southern Beijing is influenced quite significantly.

(4) As shown in 12 h $\text{PLAM}_{\rightarrow\text{BJ}}$ index prognosis chart (Figure 4(d)), the unfavorable weather condition in central Hebei has been further maintained and even aggravated. The $\text{PLAM}_{\rightarrow\text{BJ}}$ index-based predictions in rolling show that the pollutions with high index values in the southwestern Shandong province move north and they are also oriented towards Beijing.

From the above analysis, the $\text{PLAM}_{\rightarrow\text{BJ}}$ index prognosis charts describing the Beijing-oriented pollution transports

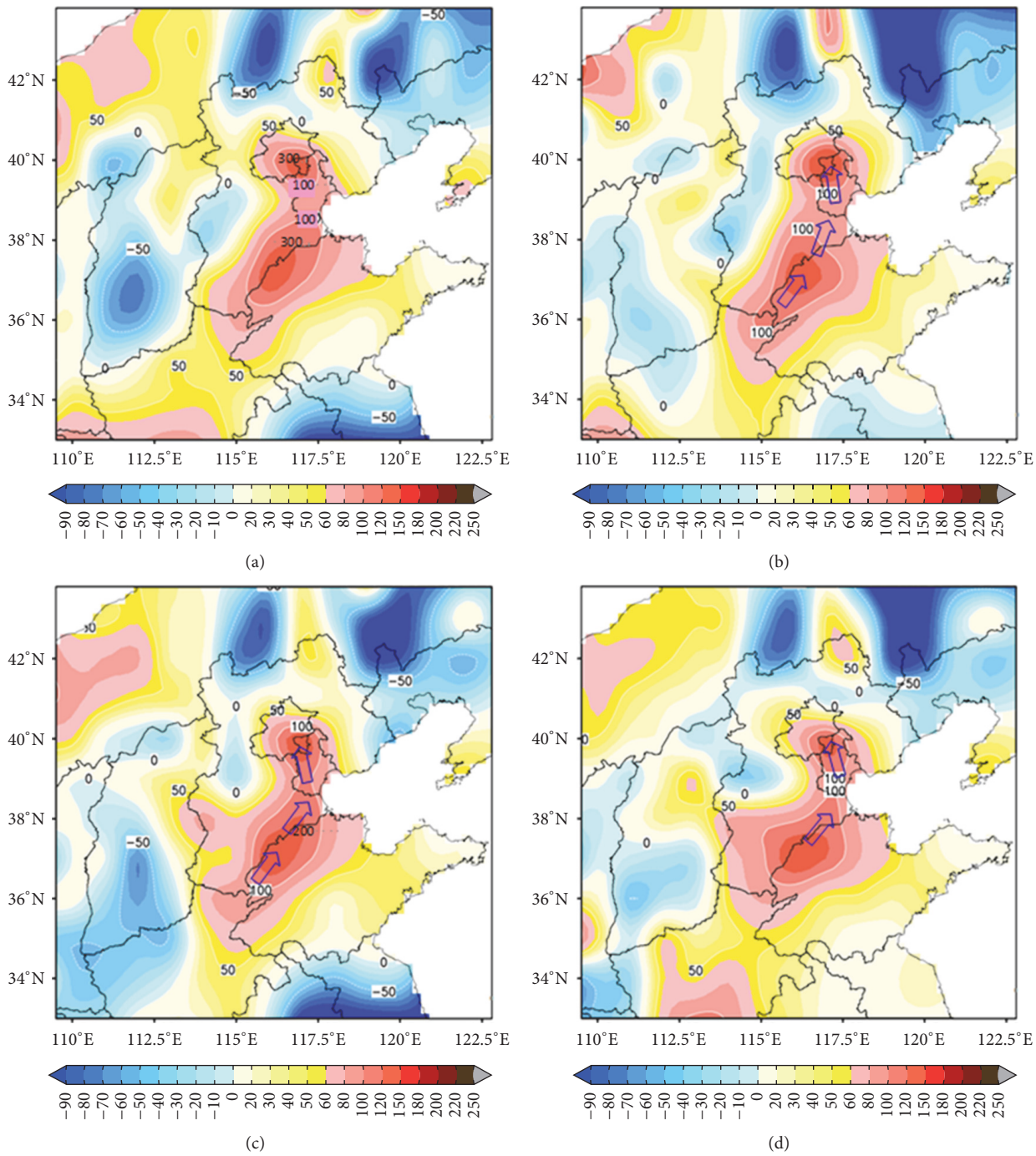

Figure 4: $PLAM_{\rightarrow BJ}$ index distribution in weather conditions on isentropic surface (280°k) at 08:00 on 20 December 2016 and 3 h (b), 6 h (c), and 12 h (d) high-resolution predictions of pollution transports oriented to Beijing from its surrounding areas. Initial time: 08:00 on 19 December; (a)–(d) are 1 h, 3 h, 6 h, and 12 h predictions.

based on nowcasting in rolling (Figures 4(b), 4(c), and 4(d)) are consistent with their actual distributions (Figure 4(a)). On one hand, this shows that the heavy pollution process over Beijing is related to pollution transports from the surrounding Hebei and western Shandong provinces. On the other hand, it also proves that PLAM index can contribute to the predictability of current refined nowcasting.

3.5. Contribution of PLAM Index to Heavy Pollution Process. Figure 5 gives an analysis on correlation of hourly day-to-day $PM_{2.5}$ measurements made in the period of 1–31 December 2016 with the PLAM index. As the figure shows, the correlation of actual $PM_{2.5}$ density with PLAM index growth is basically an e-index correlation, the correlation confirmation coefficient is given in $R^2 = 0.7324$, and its

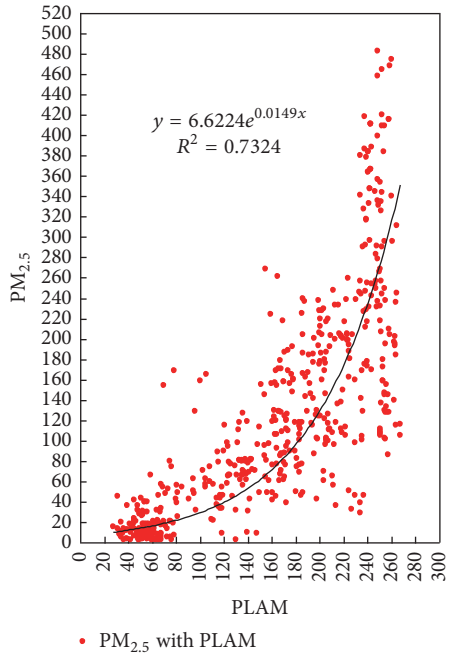

FIGURE 5: Analysis on correlation of hourly $PM_{2.5}$ measurements in Beijing in the period of 1–31 December 2016 with PLAM index under meteorological conditions.

significance level exceeds 0.001 (Figure 5). This shows that PLAM index is a meaningful indicator for aerosol accumulation and formation of heavy pollution in a specific locality, and it has the capability for quantitative diagnosis and prediction.

Overall, a composite graphic describing the heavy pollution process known as the severe hazy weather event in Beijing in December 2016 is given in Figure 6.

The meteorological conditions influencing heavy pollution in Beijing are very complicated. Based on analysis of PLAM index, this paper gives a quantitative description of basic physical attributes of the so-called static and stable atmospheric system, which provides some important clues for analyzing and diagnosing the mechanism of meteorological impacts on air pollution. An analysis on isentropic (iso-θ_e) process described by PLAM index reveals the contribution of the high-value CIN to aerosol accumulation growth in the lower atmosphere. An analysis on tracking PLAM transport index suggested that there was a pollution transport process towards Beijing from its surrounding areas. The displacement of vertical dispersion which was overlapped with the pollution transport from the adjacent areas had a significant impact and made a major contribution to forming the heavy pollution in Beijing, and it was an important factor for the aggravated and persistent hazy weather over Beijing.

3.6. The Statistical Analysis of H_PML Differences in Heavy Pollution and "Blue Sky". As we know, a large-scale haze weather occurred in the east of China, affecting an area of 1.43 million square kilometers, about 15% of the land area, during the period of 20 to 26 February in 2014. 6 consecutive heavy-polluted weather warnings were issued by China's Central Meteorological Observatory. An orange alert of heavy haze was being issued continually on 25 February in 2014. The moderate haze events occurred in Beijing, Tianjin, Hebei, Shanxi, Shandong, Henan, Shaanxi, Liaoning, and many other places; in particular, heavy haze was found in Beijing-Tianjin-Hebei and other places. In east, central, and south China, there is also a continuous haze weather. Long-lasting heavily polluted weather swept over half of China, which has a serious impact on people's production and life. In this section, we will try to analyze the significance and contribution of polluted mixed layer height in the quantitative diagnosis of large-scale haze weather system in eastern China.

In order to compare the differences of weather characteristics between the case of heavy pollution and the "blue sky" in winter, which are the two types of weather phenomena in east China, to observe the differences of the H_PML and the weather element characteristics, the weather observation reports were analyzed for the large-scale pollution cases mentioned above in eastern China for the area of the east of 100°E at 08:00 (local time), 26 February 2014. The region of eastern China, the east of 100°E are selected, from the north of Heilongjiang to the vast area of the Pearl River Delta.

The two types of extreme weather stations, "haze weather" and "Azure Sky", represented 24 and 8 sites, respectively, accounting for 6% and 2% of the total of 400 stations. The two groups of observations are listed in Tables 2 and 3. From Tables 2 and 3, we can see the following:

(1) The average situation is that there is little difference in the normal meteorological elements between medium-heavy pollution and "azure" extreme weather. For example, the differences for those two types of extreme weather are not obvious in air pressure (P), temperature (T), and wind speed; therefore, it is very limited to distinguish between haze and fine weather by using conventional meteorological elements. Only relative humidity (RH) was significantly different, for 87% and 31%, respectively. The difference for those two types of extreme weather in visibility was in 1 km and 22 km, respectively. However, the RH changes are related to various weather processes and can usually be very wide in the nonpolluted weather situation.

(2) Comparing Tables 2 and 3, it is shown that the difference of H_PML between severe pollution and "azure" extreme weather is very significant, 240 m and 1878 m on average, respectively. The H_PML for heavy pollution cases could be 8~10 times higher than "azure" weather situation. This indicates that the H_PML parameters have significant contribution to quantitative identification of the process of heavy pollution and "blue sky."

4. Conclusions

We conclude the following:

(1) As it is revealed in calculations of vertical temperature-entropy chart based on analysis of PLAM

Table 2: Observations and H_PML of heavy pollution in February 2014.

Station	Lon.	Lat.	P (hPa)	T (°C)	Wind dir. (d.)	Speed (m/s)	Vis. (km)	RH (%)	H_PML (m)	AQI level	W	$PM_{2.5}$ ($\mu g/m^3$)
Barhu	118.3	48.2	1019.7	−9	330	1	0.9	76.7	406.6	3	Rain	148.3
Shuiling	127.1	47.2	1019.9	−1	159	3	1.2	86.2	247.4	3	Fog	179
Wulan	122.1	46.1	1016	−4	205	0	0.6	73.6	492.1	3	Heavy fog	148.8
Zhao	114.7	37.5	1024.1	0	177	0	0.4	86.3	247.6	6	Heavy haze	589
Gaoyi	114.6	37.6	1023.9	0	193	0	0.9	86.3	247.6	6	Fog	589
Handan	114.7	37.0	1024.0	1	264	0	0.3	93.0	123.9	6	Heavy haze	589
Wudan	119.0	42.9	1017.4	4	248	4	2.0	60.2	865.4	5	Heavy haze	260
Fengning	116.6	41.2	1024.5	−3	293	0	1.3	86	246.8	6	Fog	456
Shunyi	116.6	40.1	1024.0	2	12	0	0.6	80.4	372.0	6	Fog	456
Huailai	115.5	40.4	1024.5	−2	0	0	0.7	86.1	247.0	6	Heavy haze	453
Chaoyang	116.5	39.9	1024.0	1	110	0	0.5	80.3	371.6	6	Heavy haze	456
Dachang	116.9	39.9	1024.0	0	13	0	0.5	86.3	247.6	6	Heavy haze	434
Beijing	116.5	39.8	1023.7	3	74	1	0.5	74.9	496.0	6	Heavy haze	434
Baoding	115.5	38.7	1023.7	1	309	0	0.7	86.4	247.9	6	Heavy haze	487
Jinghai	116.9	38.9	1023.9	4	179	1	1.4	93.2	124.4	6	Fog	453
Zhenan	109.2	33.4	1024.1	6	149	0	3.4	86.9	249.5	3	Fog	191
Yexian	113.3	33.6	1026.1	7	201	0	1.0	93.3	124.9	2	Fog	156
Miyang	113.3	32.7	1024.9	8	101	0	0.9	93.4	125.1	2	Fog	156
Laifeng	109.4	29.5	1024.4	8	9	0	1.3	100.0	5.4	2	Rain	130.5
Huarong	112.6	29.5	1025.4	9	30	0	1.3	93.4	125.2	2	Fog	148
Pingyang	120.6	27.7	1020.9	13	219	0	0.3	100	5.4	2	Heavy fog	141.4
Rui'an	120.7	27.8	1020.5	13	265	1	0.5	100	5.4	2	Heavy fog	141.4
Lianshan	112.2	24.6	1022.2	12	325	0	0.9	93.6	125.2	2	Blue sky	126
Yongding	116.72	24.73	1023.2	16	9	1	2.6	100.0	5.4	3	Rain	101.7
Average			**1023.0**	**4.0**	**161**	**1.0**	**1.0**	**87.0**	**239.7**	**4.2**		**309**

Table 3: Observations and H_PML of "Azure Sky."

Station	Lon.	Lat.	P (hPa)	T (°C)	Wind dir. (d.)	Speed (m/s)	Vis. (m)	RH ($)	H_PML (m)	AQI level	W	$PM_{2.5}$ ($\mu g/m^3$)
Dabancheng	88.3	43.4	1038	−13	69	1	30	47.1	1074	1	Blue sky	59.0
Yiwu	94.7	43.3	1041	−19	220	1	24	45.4	1061	1	Blue sky	19.5
Dingxin	99.5	40.3	1038	−10	171	1	19	13.2	2738	1	Blue sky	30.9
Dulan	98.5	36.9	1014	−4	304	2	30	22.6	2196	1	Blue sky	11.5
Xinghai	100.0	35.6	1015	−4	280	1	35	18.6	2451	1	Blue sky	5.3
Hailisu	106.0	41.4	1033	−10	247	4	17	13.2	2738	1	Blue sky	35.6
Wuzhong	106.0	38.0	1027	1	343	0	13	47	1227	2	Blue sky	44.9
Xiji	106.0	36.0	1027	−3	355	0	9	36.9	1537	2	Blue sky	60.0
Average			**1029**	**−8**	**249**	**1.3**	**22.1**	**31**	**1878**	**1**		**33.4**

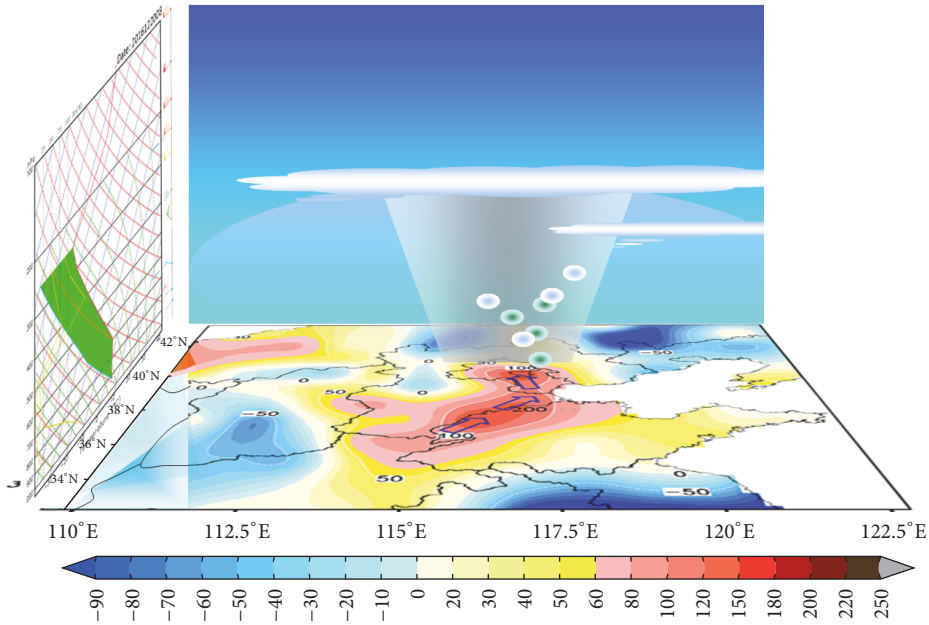

Figure 6: A physic schema shows the mechanism for forming the severe hazy weather or heavy pollution event in December 2016 in Beijing. Left section (tephigram): CIN exceeding the threshold value (shown in the green area) indicated that lowered H_PML↓ is favorable for accumulation of $PM_{2.5}$↑. Isentropic (θe) chart shows that the overlapped pollution has been transported from the surrounding areas of Beijing.

sensitive parameter θe, the ascending curve (i.e., status curve) along the iso-θe line can be represented by the blue arrow on the vertical temperature-entropy chart in Figure 6. The curve of atmospheric stratification sounding from the Beijing station is presented by a red curve in the figure. A comparison of the status curve with the sounding curve shows that the temperature T_v' of the "dirty" air parcel rising in the wet adiabatic process is far lower than its ambient air temperature Tv, with the differential reaching 7°C. Taking all this into consideration, the local CIN value in Beijing is about 50 times higher than the threshold value. As is shown in the figure, the atmosphere over Beijing area is in absolute stable status, and it is unfavorable for vertical dispersion of pollutants, thus creating a favorable condition for accumulation of $PM_{2.5}$ among other aerosols in the area.

(2) Calculations of convective condensation height in the isentropic process show that the $PM_{2.5}$ density during the heavy pollution event is inversely correlated with H_PML; the lower the H_PML is, the higher the $PM_{2.5}$ density will be. At 08:00 on 20 December 2016, the lowest H_PML value occurred, which was less than 200 meters, but the accumulated $PM_{2.5}$ was up to 500 $\mu g/m^3$. The lowered height of pollution mixing layer shows a significant positive impact on formation of severe hazy weather, eventually leading to its further aggravation and persistence. A relevant analysis on correlation of $PM_{2.5}$ observations with PLAM index shows that PLAM index is a significant indicator for aerosol accumulation and formation of heavy pollution, and it has the ability to make quantitative diagnosis and prediction.

(3) Statistical analysis of large-scale heavy polluted weather data shows that the H_PML parameters have significant contributions for quantitative identification of heavy pollution and the process of "blue sky."

(4) An analysis on tracking the $PLAM_{\rightarrow BJ}$ index on isentropic (θ_e) surface showed that the persistence and intensity increase of the heavy pollution process in Beijing were due to overlapping with the continuous high-value pollution transport from southern Hebei and western Shandong provinces. In December 2016 alone, Beijing witnessed 6 heavy pollution events and each lasted for 3–5 days, and the peaks of aerosol density in several cases are even beyond 500 $\mu g/m^3$, as overlapping with the Beijing-oriented pollution transports from its surrounding areas played an important role.

(5) The outcomes of the 3–12-hour nowcasting in rolling based on the Beijing-oriented $PLAM_{\rightarrow BJ}$ index were consistent with the actual distribution of the aerosol density. All this shows that PLAM index has certain predictability in refined nowcasting.

Conflicts of Interest

The authors declare that there are no conflicts of interest regarding the publication of this article.

Acknowledgments

This study is supported jointly by the National Key Project of MOST (2016YFC0203306) and the Basic Scientific Research Progress of the Chinese Academy of Meteorological Sciences (2016Z001), the National Key Project of Basic Research

(2014CB441201, 453172), and the National Natural Science Foundation of China (Grant no. 41475097).

References

[1] X. Y. Zhang, Y. Q. Wang, and T. Niu, "Atmospheric aerosol compositions in China: spatial/temporal variability, chemical signature, regional haze distribution and comparisons with global aerosols," *Atmospheric Chemistry and Physics*, vol. 12, no. 2, pp. 779–799, 2012.

[2] R. Liu and Z. Han, "The Effects of Anthropogenic Heat Release on Urban Meteorology and Implication for Haze Pollution in the Beijing-Tianjin-Hebei Region," *Advances in Meteorology*, vol. 2016, Article ID 6178308, 2016.

[3] Y. Li, W. Wang, J. Wang, X. Zhang, W. Lin, and Y. Yang, "Impact of air pollution control measures and weather conditions on asthma during the 2008 Summer Olympic Games in Beijing," *International Journal of Biometerology*, vol. 55, no. 4, pp. 547–554, 2011.

[4] Y. Ao, J. Li, Z. Li, S. Lyu, C. Jiang, and M. Wang, "Relation between the Atmospheric Boundary Layer and Impact Factors under Severe Surface Thermal Conditions," *Advances in Meteorology*, vol. 2017, pp. 1–12, 2017.

[5] C. Honoré, L. Rouïl, R. Vautard et al., "Predictability of European air quality: Assessment of 3 years of operational forecasts and analyses by the PREV'AIR system," *Journal of Geophysical Research: Atmospheres*, vol. 113, no. 4, Article ID D04301, 2008.

[6] S. L. Gong, L. A. Barrie, J. P. Blanchet, K. V. Salzen, U. Lohmann, and G. Lesins, "Canadian Aerosol Module: A size-segregated simulation of atmospheric aerosol processes for climate and air quality models 1," *Journal of Geophysical Research Atmospheres*, vol. 108, pp. 10–22, 2003.

[7] J. Wang, Y. Wang, H. Liu et al., "Diagnostic identification of the impact of meteorological conditions on PM2.5 concentrations in Beijing," *Atmospheric Environment*, vol. 81, pp. 158–165, 2013.

[8] H. L. Kuo, "Further studies on the parameterization of the influence of cumulus convection in large-scale flows," *Journal of Atmospheric Sciences*, vol. 31, pp. 1232–1240, 1974.

[9] X.-M. Hu, J. Huang, J. D. Fuentes, R. Forkel, and N. Zhang, "Advances in Boundary-Layer/Air Pollution Meteorology," *Advances in Meteorology*, vol. 2016, Article ID 2825019, 2016.

[10] X. Y. Zhang, Y. Q. Wang, W. L. Lin et al., "Changes of atmospheric composition and optical properties over beijing 2008 olympic monitoring campaign," *Bulletin of the American Meteorological Society*, vol. 90, no. 11, pp. 1633–1651, 2009.

[11] N. L. Bindoff, P. A. Stott, and K. M. AchutaRao, "Detection and Attribution of Climate Change: from Global to Regional," in *Climate Change 2013: The Physical Science Basis. Contribution of Working Group I to the Fifth Assessment Report of the Intergovernmental Panel on Climate Change*, T. F. Stocker, D. Qin, G.-K. Plattner et al., Eds., Cambridge University Press, Cambridge, UK, 2013, The Physical Science Basis.

[12] Y. Q. Yang, J. Z. Wang, and Q. Hou, "A plam index for Beijing stabilized weather forecast in summer over Beijing," *Journal of Applied Meteorological Science*, vol. 20, pp. 649–659, 2009.

[13] J. Z. Wang, S. L. Gong, X. Y. Zhang et al., "A parameterized method for air-quality diagnosis and its applications," *Advances in Meteorology*, vol. 2012, Article ID 238589, 2012.

[14] J. Z. Wang, L. G. Bian, and C. D. Xiao, "Dynamics of Ekman boundary layer over the Antarctic plateau in Summer," *Chinese Science Bulletin*, vol. 59, pp. 999–1005, 2014.

[15] G. Zhang, L. Bian, J. Wang, Y. Yang, W. Yao, and X. Xu, "The boundary layer characteristics in the heavy fog formation process over Beijing and its adjacent areas," *Science China Earth Sciences*, vol. 48, no. 2, pp. 88–101, 2005.

[16] D. A. Haugen, J. C. Kaimal, and E. F. Bradley, "An experimental study of Reynolds stress and heat flux in the atmospheric surface layer," *Quarterly Journal of the Royal Meteorological Society*, vol. 97, no. 412, pp. 168–180, 1971.

[17] J. M. Wallace and P. V. Hobbs, "Atmospheric science, "an introductory survey"," *Elsevier*, p. 486, 2006.

[18] J. Zhao, "A simulative study of the thermal mechanism for development of the convective boundary layer in the arid zone of northwest China," *Acta Meteorologica Sinica*, vol. 69, no. 6, pp. 1029–1037, 2011.

[19] Q. Zhang, G. A. Wei, and P. Hou, "Observation studies of atmosphere boundary layer characteristic over Dunhuang gobi in early summer," *Plateau Meteorology*, vol. 23, no. 5, pp. 587–597, 2004.

[20] Y. Ma, M. Menenti, and R. Feddes, "Parameterization of heat fluxes at heterogeneous surfaces by integrating satellite measurements with surface layer and atmospheric boundary layer observations," *Advances in Atmospheric Sciences*, vol. 27, no. 2, pp. 328–336, 2010.

[21] D. S. Yang, Y. B. Yu, and S. K. Liu, "Meteorological dynamics," *Beijing: Meteorological Press*, pp. 297–422, 1983.

[22] S. Gao, Y. Zhou, T. Lei, and J. Sun, "Analyses of hot and humid weather in Beijing city in summer and its dynamical identification," *Science China Earth Sciences*, vol. 48, no. 2, pp. 128–137, 2005.

[23] J. Z. Wang and Y. Q. Yang, "Modern Weather Engineering Beijing," *Meteorological Press*, pp. 334–339, 2000.

[24] D. V. Spracklen, K. S. Carslaw, M. Kulmala et al., "Contribution of particle formation to global cloud condensation nuclei concentrations," *Geophysical Research Letters*, vol. 35, no. 6, Article ID L06808, 2008.

[25] M. A. Shapiro, "The use of isentropic coordinates in the formulation of objective analysis and numerical prediction models," *Atmosphere*, vol. 12, no. 1, pp. 10–17, 1974.

[26] M. A. Shapiro and J. T. Hastings, "Objective cross-section analysis by Hermite polynomial interpolation on isentropic surfaces," *Journal of Applied Meteorology*, vol. 12, pp. 753–762, 1973.

[27] J. Z. Wang, "Study on heavy snow in North China for December 2, 1974," *Journal of Atmospheric Sciences, Sinica*, vol. 2, no. 4, pp. 307–313, 1978.

[28] K. A. Browning, M. E. Hardman, T. W. Harrold, and C. W. Pardoe, "The structure of rainbands within a mid-latitude depression," *Quarterly Journal of the Royal Meteorological Society*, vol. 99, no. 420, pp. 215–231, 1973.